Journal of Clinical and Translational Hepatology **2021** vol. 9(6) | 917–930
DOI: 10.14218/JCTH.2021.00032

Original Article

Indole-3-propionic Acid-aggravated CCl_4-induced Liver Fibrosis via the TGF-β1/Smads Signaling Pathway

Fei Liu[#], Changfeng Sun[#], Yuanfang Chen, Fei Du, Yuxiang Yang and Gang Wu[*]

Department of Infectious Diseases, Department of Tuberculosis, Laboratory of Infection and Immunity, The Affiliated Hospital of Southwest Medical University, Luzhou, Sichuan, China

Received: 18 January 2021 | **Revised:** 24 March 2021 | **Accepted:** 7 April 2021 | **Published:** 17 May 2021

Abstract

Background and Aims: The pathogenesis of liver fibrosis involves liver damage, inflammation, oxidative stress, and intestinal dysfunction. Indole-3-propionic acid (IPA) has been demonstrated to have antioxidant, anti-inflammatory and anticancer activities, and a role in maintaining gut homeostasis. The current study aimed to investigate the role of IPA in carbon tetrachloride (CCl_4)-induced liver fibrosis and explore the underlying mechanisms. ***Methods:*** The liver fibrosis model was established in male C57BL/6 mice by intraperitoneal injection of CCl_4 twice weekly. IPA intervention was made orally (20 mg/kg daily). The degree of liver injury and fibrosis were assessed by serum alanine aminotransferase (ALT), aspartate aminotransferase (AST), and histopathology. Enzyme-linked immunosorbent assay and quantitative real-time polymerase chain reaction (qPCR) were used to detect the inflammatory cytokines. The malondialdehyde (MDA), glutathione, glutathione peroxidase, superoxide dismutase, and catalase were determined via commercial kits. Hepatocyte apoptosis was detected by terminal deoxynucleotidyl transferase-mediated dUTP nick end labeling assay. The expression of mRNA and protein was assayed by qPCR, Western blotting, or immunohistochemical staining. ***Results:*** After IPA treatment, the ALT and AST, apoptotic cells, and pro-inflammatory factor levels were enhanced significantly. Moreover, IPA intervention up-regulated the expression of collagen I, α-smooth muscle actin, tissue inhibitor of matrix metalloproteinase-1, matrix metalloproteinase-2, transforming growth factor-β1 (TGF-β1), Smad3, and phosphorylated-Smad2/3. Additionally, IPA intervention did not affect the MDA level. Attractively, the administration of IPA remodeled the gut flora structure. ***Conclusions:*** IPA aggravated CCl_4-induced liver damage and fibrosis by activating HSCs via the TGF-β1/Smads signaling pathway.

Citation of this article: Liu F, Sun C, Chen Y, Du F, Yang Y, Wu G. Indole-3-propionic acid-aggravated CCl_4-induced liver fibrosis via the TGF-β1/Smads signaling pathway. J Clin Transl Hepatol 2021;9(6):917–930. doi: 10.14218/JCTH.2021.00032.

Introduction

Liver fibrogenesis is a typical pathological process in the development of almost all chronic liver diseases (CLDs).[1] It has been confirmed that late-stage liver fibrosis is irreversible and may result in cirrhosis or hepatocellular carcinoma (commonly referred to as HCC).[2] Accumulated evidence have suggested that the key step of liver fibrosis involves the activation of hepatic stellate cells (HSCs) and excessive accumulation of extracellular matrix (ECM) proteins.[3] During chronic liver injury, HSCs can be directly or indirectly activated by various factors (*e.g.*, injured epithelial cells,[2] reactive oxygen species [commonly referred to as ROS], growth factors, inflammatory cytokines,[4] enteric dysbiosis,[2,5] etc.) and express a large amount of ECM-related proteins to promote liver fibrosis.[6] In the process of liver fibrosis, transforming growth factor-β (TGF-β) is considered a critical mediator that is involved in various processes, such as HSC activation, inflammatory immunity, and apoptosis.[5] Generally, TGF-β exerts biological effects via the Smads signaling pathway.[7] In the Smads signaling pathway, Smad2/Smad3 has been identified as the crucial inducer of liver fibrogenesis, whereas Smad7 acts as a suppressor.[7,8] Therefore, removing the factors that induce the activation of HSCs and inhibiting the activation of HSCs and TGF-β/Smads signaling may be a promising approach to treating liver fibrosis. Impaired gut barrier and dysregulated gut microbiota also often occur in CLD.[9] The microbiota-gut-liver axis may, therefore, be a potential target for the prevention and treatment of the progression of CLD.

Indole-3-propionate (IPA) is a metabolite produced by gut symbionts, such as *Clostridium Sporogenes* (*C. Sporogenes*), metabolizing tryptophan, and is considered as a natural compound with clinical application value. It has been demonstrated that IPA can alleviate the pathophysiological process of various diseases (*e.g.,* chronic kidney

Keywords: Indole-3-propionic acid; CCl_4; Hepatic fibrosis; HSCs; TGF-β1.

Abbreviations: α-SMA, α-smooth muscle actin; AHR, aryl hydrocarbon receptor; ALT, alanine aminotransferase; AST, aspartate aminotransferase; CAT, catalase; CCl_4, carbon tetrachloride; CLD, chronic liver disease; ECM, extracellular matrix; EHC, enterohepatic circulation; ELISA, enzyme-linked immunosorbent assay; GSH, glutathione; GSH-PX, glutathione peroxidase; HCC, hepatocellular carcinoma; HFD, high-fat diet; HSCs, hepatic stellate cells; IHC, immunohistochemistry; IL, interleukin; IPA, indole-3-propionate; LPS, lipopolysaccharide; MDA, malonyldialdehyde; MMPs, matrix metalloproteinases; NAFLD, non-alcoholic fatty liver; OTUs, Operational Taxonomic Units; PXR, pregnane X receptor; qPCR, quantitative real-time polymerase chain reaction; ROS, reactive oxygen species; SOD, superoxide dismutase; TGF-β, transforming growth factor-β; TIMPs, tissue inhibitors of metalloproteinase; TNF-α, tumor necrosis factor-α; TUNEL, terminal deoxynucleotidyl transferase-mediated dUTP nick end labeling.

[#]Contributed equally to this work.

[*]**Correspondence to:** Gang Wu, Department of Infectious Disease, The Affiliated Hospital of Southwest Medical University, Luzhou, Sichuan 646000, China. ORCID: https://orcid.org/0000-0002-2513-5089. Tel/Fax: +86-830-3165-625, E-mail: wugang2020@swmu.edu.cn

disease, Alzheimer's disease, cancer) which rely on its multiple biological effects.[10–12] Sonnenburg *et al*.[13] found that compared with the sterile mice injected with wild-type *C. Sporogenes*, mice injected with fldC-deficient bacteria have significantly lower serum IPA levels, weaker immune activity, increased intestinal permeability, and often showed inflammatory bowel disease. IPA can directly decrease intestinal permeability by the pregnane X receptor (PXR) to increase the stability of the intestinal mucosa,[14] and administration of IPA can modulate the microbiota composition and inhibit gut dysbiosis of rats induced by a high-fat diet (referred to as HFD).[15] Moreover, IPA can be absorbed into the bloodstream through intestinal epithelium to exert antioxidative and anti-inflammatory effects.[16] Research shows that IPA can directly decrease the expression of lipopolysaccharide (LPS)-induced proinflammatory cytokines, including tumor necrosis factor-α (TNF-α), interleukin (IL)-1β and IL-6 via inhibition of the NF-κB signaling pathway in hepatic macrophages.[15]

There are conflicting results for the effects of IPA on host oxidative stress, obtained by different experiments. Previous studies have shown that IPA acts as an effective natural free radical scavenger *in vivo*[10] and cannot be converted to reactive intermediates with pro-oxidative activity;[11] it can also synergize with the well-known intracellular antioxidant glutathione (GSH).[17] Thus, IPA can protect against oxidative damage and lipid peroxidation in the brain,[17] kidney,[10] and liver.[18] However, it was found in another study that IPA has cytostatic properties in breast cancer by inducing oxidative stress and activating aryl hydrocarbon receptor (AHR) and PXR receptors,[12] which indicates that there are certain differences in the effects of IPA on oxidative stress in different conditions. Recently, it has been reported that IPA has the ability to reduce HFD-induced liver fibrosis by inhibiting the expression levels of such fibrogenic genes as TGF-β, α-smooth muscle actin (α-SMA), and such collagen synthetic genes as Col1α1, Col1α2, and Col3α1.[15]

Therefore, we speculated that the compound might inhibit liver fibrosis caused by free radical damage and chronic inflammation, and relieve intestinal dysfunction related to CLD. In this investigation, CCl_4-induced liver fibrosis, the commonly used experimental model for inducing toxin-mediated liver fibrosis,[19] was adopted to evaluate the effect of IPA on liver fibrosis and elucidate the potential mechanism.

Methods

Liver fibrosis model

Specific pathogen-free male C57BL/6 mice weighing about 25g at 6–8 weeks of age were purchased from Dossy Experimental Animals CO., LTD. (Chengdu, China) and raised under the pathogen-free condition at 22±2°C with a 12-h light/dark cycle and free access to sterile water and laboratory chow. Mice were acclimated to the requirements for 1 week before animal experiments and randomly divided into the following four groups (Supplementary Table 1): normal control (n=3); IPA control (n=3); CCl_4 model (n=3); and, IPA intervention (n=4).

The mice in the CCl_4 model group and IPA intervention group were used to induce liver fibrosis by intraperitoneal injection of 5 μL/g body weight 10% (v/v) CCl_4 (dissolved in olive oil) two times per week for 8 weeks.[19] The mice in the normal control group and IPA control group were injected with olive oil (5 μL/g body weight) two times per week for 8 weeks. According to the previous report,[15] oral IPA at a dose of 20 mg/kg/day can alleviate liver injury caused by HFD and produce no adverse reactions. Therefore, we used the same dose in this study. The IPA control group and IPA intervention group were treated with oral gavage IPA solution (20 mg/kg/day) once daily for 8 weeks according to the previous report,[15] the normal control and the CCl_4 model group were treated with vehicle (20 mg/kg/day) once daily for 8 weeks. IPA (GI0540) was purchased from G-Clone Biotechnology Co. Ltd (Beijing, China). Preparation of the IPA solution was carried out as previously described.[17]

This study was approved by the Institutional Animal Ethics Committee of the Affiliated Hospital of Southwest Medical University (Luzhou, China).

Tissue sample processing and histopathological evaluation

Liver tissues were fixed with 4% paraformaldehyde for 24–48 h and embedded in paraffin wax. The paraffin blocks were cut into 4-μm tissue sections and mounted on glass slides. Histological assessment of the liver tissue sections was performed following hematoxylin-eosin staining and Masson's trichrome staining, as previously described according to previous methods.[20] The collagen accumulation in livers was examined by Masson's trichrome staining and quantified by ImageJ Analyzer. According to the Ishak score system,[21] the degree of liver damage was evaluated blindly by two pathologists under a light microscope.

Biochemical analysis of the liver function

Serum samples were obtained by centrifugation at 3,000 rpm for 10 m. Then, the biochemical indicators, including aspartate aminotransferase (AST), alanine aminotransferase (ALT), total bilirubin, total bile acid, cholesterol, and triglycerides were detected via the Automated Biochemical Analyzer (ADVIA 2400; Siemens Healthineers, Cary, NC, USA).

Immunohistochemistry (referred to as IHC) staining

Before immunostaining, paraffin-embedded sections were dewaxed and rehydrated in an alcohol series. The sections were washed with phosphate-buffered saline after heat-induced antigen retrieval. Next, the sections were treated with 3% hydrogen peroxide for 15 m to eliminate endogenous peroxidase activity and then incubated with 3% bovine serum albumin for 30 m at 37°C to block non-specific binding sites. Subsequently, sections were incubated overnight at 4°C with diluted primary antibodies, including α-SMA (1:2,000; GB13044; Servicebio, Inc. Wuhan, China), collagen I (1:1,200; GB11022-3; Servicebio, Inc.), matrix metalloproteinase (MMP)-2 (1:1,200; GB11130; Servicebio, Inc.), tissue inhibitors of metalloproteinase-1 (TIMP-1) (1:1,000; 106164-T40; Sino Biological US, Chesterbrook, PA, USA), TGF-β1 (1:500; GB11179; Servicebio, Inc.), and incubated with a conjugated secondary antibody after washing with phosphate-buffered saline (G0002; Servicebio, Inc.). Diaminobenzidine kits (G1211; Servicebio, Inc.) were used to visualize antibody binding areas. For each mouse, we analyzed three liver slices and randomly observed the positive-stained areas in three different fields of vision on each slice. The ratio of positive-stained to total area was calculated by Image-Pro Plus 6.0.

Enzyme-linked immunosorbent assay (ELISA)

The level of IPA, LPS in serum, and concentration of TNF-α,

IL-1β, IL-10 and TGF-β1 in the liver tissues were determined by ELISA, following the manufacturers' respective protocols. LPS ELISA kit (SEB526Ge) was purchased from USCN KIT INC (Wuhan, China). TNF-α (88-7324-88), IL-1β (CSB-E04726m) ELISA kits were purchased from Thermo Fisher Scientific Institute (Cleveland, OH, USA). TGF-β1 ELISA kit (CSB-E04726m) was purchased from CUSABIO Co. Ltd (Wuhan, China). IL-10 ELISA kit was purchased from MultiSciences Biotech Co., Ltd (Hangzhou, China). IPA ELISA kit (ml058187) was purchased from Enzyme-linked Biotechnology Co. Ltd (Shanghai, China).

Assessment of oxidative stress and lipid peroxidation

To assess the degree of oxidative stress and lipid peroxidation, the levels of malondialdehyde (MDA), GSH, glutathione peroxidase (GSH-Px), superoxide dismutase (SOD), and catalase (CAT) in liver tissue were detected by commercially available kits, according to the manufacturer's instructions. These commercially available kits were purchased from Nanjing Jiancheng Bio-engineering Institute (Nanjing, China).

Apoptosis detection by TdT-mediated dUTP nick-end labeling (TUNEL) staining

According to the manufacturer's protocol, apoptosis cells in the paraffin-embedded liver sections were detected by a TUNEL assay kit (Vazyme, Wuhan, China).[22] Microscopic examination and collecting images were performed through a fluorescence microscope. The results showed the nucleus to be blue upon labeling with 4′,6-diamidino-2-phenylindole reagent (Vazyme) and positive apoptosis cells to be green.

Quantitative real-time polymerase chain reaction (qPCR)

Total RNA was extracted from liver tissues using Trizol reagent (G-Clone, Beijing, China) and reverse transcribed into cDNA by HiScript III RT SuperMix (Vazyme) for qPCR with gDNA wiper, following the manufacturer's instruction. The mRNA levels of α-SMA, collagen-1, MMP-2, TIMP-1, TGF-β1, Smad3, Smad7, TNF-α, IL-6, IL-8, and IL-10 were detected using AceQ qPCR SYBR Green Master Mix (Vazyme) performed on StepOne Plus Real-Time PCR System (Applied Biosystems, Hercules, CA, USA). GAPDH was used as an internal control. Relative expression of target gene mRNA calculated using the $2^{-\Delta Ct}$ method.[23] Primers used in this study are listed in Supplementary Table 2.

Western blotting

Total protein was extracted from liver tissue using radioimmunoprecipitation assay lysis buffer (Servicebio, Inc.) following the manufacturer's protocol. After centrifugation, the concentration of total protein was determined using a bicinchoninic acid protein assay kit (Servicebio, Inc.). After mixing the protein samples with sodium dodecyl sulfate-polyacrylamide gel electrophoresis sample loading buffer (5) at a ratio of 4:1, they were boiled for 15 m to denature the protein. The samples were then separated on 10% sodium dodecyl sulfate-polyacrylamide gels (Servicebio, Inc.) and transferred onto polyvinylidene fluoride membranes (Millipore, Bedford, MA, USA). The membranes were blocked with 5% skim milk powder at room temperature for 1 h and incubated at 4°C overnight with the following primary antibodies: ACTIN (1:1,000; Servicebio, Inc.), phosphorylated (p)-Smad2/3 (1:1,000; Bioworld Technology, Inc., St Louis Park, MN, USA), Smad7 (1:1,000; Servicebio, Inc.), and then were incubated with fluorescence-labeled rabbit anti-goat IgG (1:5,000; Servicebio, Inc.) for 30 m at room temperature. The protein band intensities were detected by AlphaEase FC software (Alpha Innotech, San Leandro, CA, USA).

Fecal measurements

Before the intervention and at 8 weeks after the intervention, we collected mouse fecal samples immediately upon defecation and stored them at −80°C. Fecal DNA was extracted from the fecal samples using the CTAB method.[24] The extracted DNA was diluted to a concentration of 1 μg/μL after detecting the purity and quantity. The V3–V4 region of the bacterial 16S ribosomal RNA was amplified by PCR. The PCR products were mixed in equal amounts, and the target strips recovered using a gel recovery kit. The library was constructed using the TruSeq® DNA PCR-Free Sample Preparation Kit (Illumina, San Diego, CA, USA), according to the manufacturer's instructions. The constructed library was quantified by Qubit and qPCR, and the qualified library was sequenced using the NovaSeq6000. According to the barcode sequence and PCR amplification primer sequence, the data of each group of samples are separated from the offline data. The raw tags data (Raw Tags) were assembled from the reads of each sample using FLASH, after the barcode and primer sequences were truncated, and the Raw Tags were filtered and processed to high-quality Tags data (Clean Tags). The obtained tags were removed from the chimera sequence to obtain the final effective data (Effective Tags) according to the tags quality control process of Qiime. Effective Tags were clustered using Uparse software (sequences with 97% consistency are clustered into Operational Taxonomic Units [OTUs]). Simultaneously, the sequences with the highest occurrence frequency in OTUs were selected as OTUs, according to the algorithm principles. The species annotations of the OTUs sequence were obtained with the Mothur method and SSUrRNA database of SILVA138 (threshold value 0.8~1).[25,26] Taxonomic information was obtained by counting the community composition of each sample at the phylum and genus levels, and MUSCLE software was used to analyze the phylogenetic relationship of all OTUs representative sequences. Alpha Diversity and Beta Diversity were used to analyze the microbial community diversity of the within-community composition of different groups.

Statistical analysis

All data were expressed as mean±standard error of the mean and analyzed using SPSS25.0 or Prism GraphPad 5.0. A two-tail Student's *t* test was applied to assess the differences between groups. A p value <0.05 was considered statistically significant.

Results

IPA aggravated liver damage and liver fibrosis in CCl_4-treated mice

As shown in Figure 1A, livers in the normal control and IPA control group showed a smooth surface with uniform color

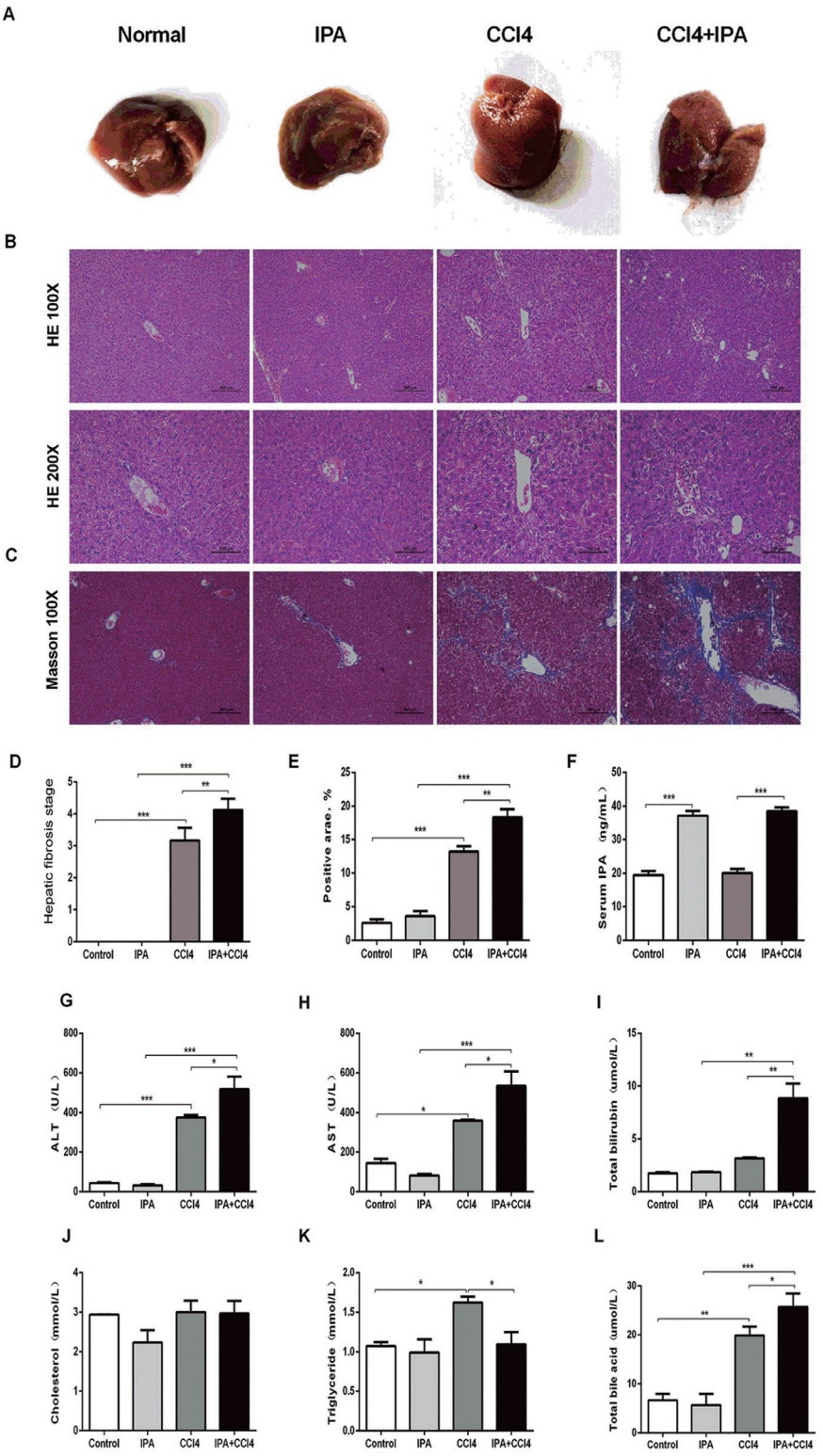

Fig. 1. Effect of IPA intervention on CCl_4-induced liver injury. (A) Fresh liver of each group of mice. (B–C) Hematoxylin-eosin-stained liver tissues (magnification 100× and 200× respectively) and Masson trichrome staining of liver tissues (magnification 100×). (D) ELISA-quantified serum levels of IPA. (E) Hepatic fibrosis stages of mice analyzed according to the Ishak histological activity index. (F) Semi-quantification data for relative fibrosis levels expressed as the positive area of the total liver area. (G–F) Automatic biochemical analyzer-estimated ALT, AST, total bilirubin (TBIL), cholesterol, triglycerides, and total bile acid (TBA) in mouse sera. All values are expressed as the mean± standard error of the mean (SEM). n=3 or 4. *p<0.05, **p<0.01, ***p<0.001. Error bars indicate the SEM. ALT, alanine aminotransferase; AST, aspartate aminotransferase; CCl_4, carbon tetrachloride; ELISA, enzyme-linked immunosorbent assay; IPA, indole-3-propionate.

and almost no adhesion to surrounding tissues, while the livers in the CCl_4-treated mice featured noticeable fine particles on the surface and serious adhesions with surrounding tissues. These visible lesions were more evident after IPA intervention. Morphological and histological changes in the liver sections revealed by hematoxylin-eosin and Masson staining indicated that CCl_4 could result in hepatocyte necrosis, inflammatory infiltrates, disruption, and reconstruction of the hepatic lobule structure. Moreover, the extent of liver tissue pathological changes seemed to be more serious in the IPA intervention group (Fig. 1B–C). The results of the quantitative analysis also demonstrated that the ratio of fibrosis score and collagen deposition positive area in the IPA intervention group increased significantly mor than in the CCl_4 model group (Fig. 1D–E). Consistent with histopathological changes, serum ALT and AST activities, as indicators of liver injury, increased after CCl_4 treatment and increased more significantly after IPA intervention (Fig. 1G–H). Interestingly, serum AST and ALT and pathological changes of liver tissue had no significant difference between the IPA control group and the normal control group (Fig. 1A–H), although serum IPA increased after IPA treatment (Fig. 1F), which proved that oral IPA alone cannot cause liver damage and liver fibrosis, but IPA plus CCl_4 would aggravate liver damage and promote liver fibrosis in CCl_4-induced mice. Besides, IPA intervention did not affect cholesterol but could markedly reduce serum triglycerides and increase the serum total bilirubin and total serum bile acid (Fig. 1J–K).

IPA enhanced hepatic inflammation in CCl_4-treated mice

The chronic inflammatory response is closely related to liver fibrosis. To assess the effect of IPA on hepatic inflammation induced by CCl_4, inflammatory cytokines were detected by qPCR and ELISA. As expected, compared with the normal control group, inflammatory cytokines in liver tissue, including IL-6, IL-8, IL-1β, IL-10, and TNF-α were significantly elevated after CCl_4 treatment. The above pro-inflammatory mediators, including IL-6, IL-8, IL-1β and TNF-α, were further enhanced and anti-inflammatory cytokines (IL-10) declined obviously after IPA plus CCl_4 treatment (Fig. 2A–G).

Considering that CLD often triggers dysbacteriosis,[9] resulting in endotoxins such as LPS moving into the portal vein and subsequently contributing to higher inflammation response. Therefore, we tested the level of serum LPS, but there was no difference between the four groups (Fig. 2H), which was consistent with findings from other studies indicating that there was no increase in circulating LPS concentration in CCl_4-treated mice.[27] These results indicated that the increased inflammation response caused by IPA may not be mediated by LPS.

Effect of IPA intervention on CCl_4-induced hepatic oxidative stress in liver

Oxidative stress is an imbalance status between the oxidant generation and the antioxidant systems and is an important causative factor of CCl_4-induced liver damage. GSH, SOD, GSH-Px, and CAT are essential participants in removing ROS. MDA is considered an indicator of lipid peroxidation. Hence, we measured antioxidants (GSH, SOD, GSH-Px, CAT) and MDA in the liver to evaluate CCl_4-induced oxidative stress. The results showed that CCl_4 treatment remarkably reduced GSH, SOD, GSH-Px, CAT, and augmented MDA in the liver (Fig. 3A–E). Notably, administration of IPA alone did not affect the level of hepatic MDA and antioxidants under normal conditions. However, compared with the CCl_4 model group, CCl_4 plus IPA intervention can further elevate the CAT activity (Fig. 3E), reduce the levels of GSH contents and GSH-PX activity (Fig. 3B–C), and produce no significant effect on MDA and the activity of SOD (Fig. 3A, D). Inconsistent with previous conclusions, this result indicated that IPA could not reduce the lipid peroxidation damage induced by CCl_4, which may be due to the different effects of IPA on oxidative stress under different conditions.

Effect of IPA intervention on hepatocyte apoptosis in mice induced by CCl_4

To discover the mechanism of IPA exacerbating the liver injury, we used TUNEL staining to detect apoptotic cells in the liver (Fig. 4A–D). In the normal control group and the IPA control group, only a few cells undergo apoptosis (Fig. 4A, B). As shown in Figure 4E, the number of hepatocyte apoptosis in the CCl_4 treatment group increased, while the IPA intervention group had a higher apoptotic rate, which suggested that oral IPA might aggravate CCl_4 induced-liver damage by promoting hepatocyte apoptosis.

IPA promoted the activation of HSCs induced by CCl_4

The extensive activation of HSCs is a typical feature of liver fibrosis, and it will cause abnormal deposition of ECM components, such as collagen I and α-SMA, and influence the synthesis and degradation of TIMP-1 and MMP-2. Among these, α-SMA and collagen-I are the most commonly used as specific expression genes for indication of HSC activation.[2] IHC and qPCR were used to detect the levels of the above molecules in liver tissues. We found that compared with the normal control group, collagen I, α-SMA, TIMP-1, and MMP-2 were significantly up-regulated in transcription and translation levels in the CCl_4-treated mice (Fig. 5A–B), while these indicators increased more obviously in the IPA intervention group (Fig. 5B–E). This result indicated that IPA enhanced the excessive deposition of ECM by aggravating the activation of HSCs.

TGF-β1/Smads signaling was associated with IPA-aggravated liver fibrosis

The TGF-β1/Smads signaling pathway plays a key role in the fibrogenic response of HSCs to CCl_4.[7] TGF-β1 detected by IHC, ELISA, and qPCR showed that TGF-β1 was significantly increased in CCl_4-treated mice and further enhanced after IPA intervention (Fig. 6A–C). Western blotting and qPCR were used to detect downstream related proteins. The results showed that after CCl_4 treatment, the Smad3 mRNA and p-Smad2/3 increased, while after CCl_4 plus IPA intervention, the levels of the above indicators increased more significantly (Fig. 6E–G). It is worth noting that the expression of Smad7 mRNA and protein was suppressed in the IPA intervention group compared with other groups (Fig. 6D, H). These preliminary results indicated that IPA might activate HSCs via the TGF-β1/Smads signaling pathway.

Effect of oral IPA on gut microbiota in CCl_4-induced liver fibrosis

To explore the potential impact of IPA on the gut microbial community in CCl_4-induced liver fibrosis, we collected fecal samples for 16S rRNA gene sequencing. The results showed that oral IPA could significantly alter the structure of intesti-

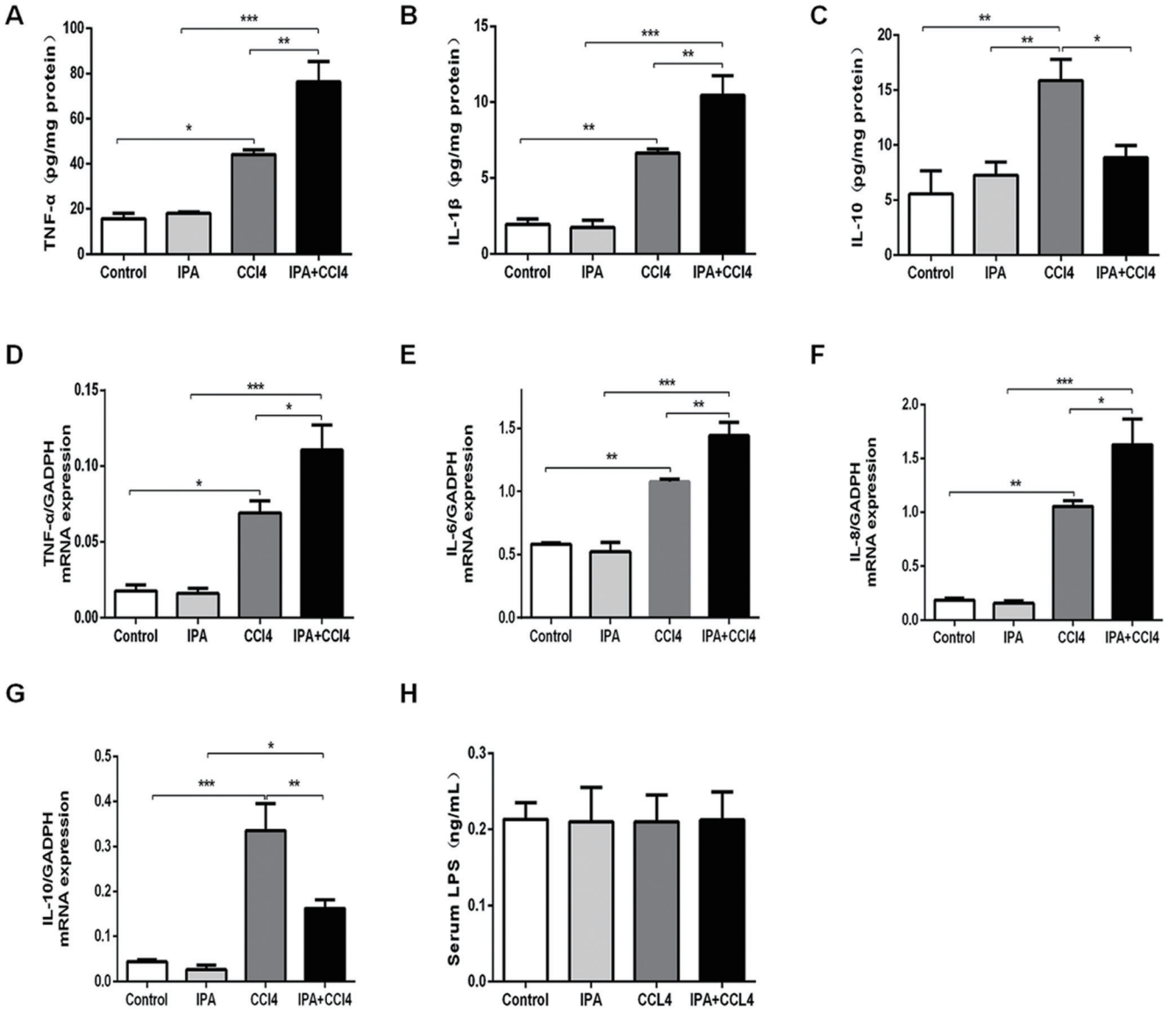

Fig. 2. IPA enhanced hepatic inflammation in CCl_4-treated mice. (A–C) ELISA was performed to detect the protein concentrations of TNF-α, IL-10, and IL-1β in liver tissue. (D–G) Relative mRNA levels of TNF-α, IL-6, IL-8, and IL-10. The level of IL-1β failed to reach the minimum detection limit of qPCR. (H) ELISA-detected serum LPS level. All values were assessed by two independent experiments; the values represent the mean±SEM. n=3–4. *p<0.05, **p<0.01, ***p<0.001. α-SMA, CCl_4, carbon tetrachloride; ELISA, enzyme-linked immunosorbent assay; IL, interleukin; IPA, indole-3-propionate; LPS, lipopolysaccharide; qPCR, quantitative real-time polymerase chain reaction; TNF-α, tumor necrosis factor-α.

nal flora in CCl_4-treated liver fibrosis mice. As shown in Figure 7A, we selected the top 35 genera based on the species annotation and abundance information of the samples and then clustered them at the species and sample levels, and found that there were significant differences in the degree of species aggregation in the feces of each group. Then, we assessed the gut microbial profile at the phylum level. In the CCl_4 model group, the abundance of *Firmicutes* was enormously increased and of *Bacteroidetes* was decreased, while this change was reversed by IPA intervention (Fig. 7B). It is worth mentioning that the two pro-inflammation-related genera *Desulfobacterota*[28] and *Campilobacterota*[29] were almost absent in other groups but were significantly increased in the IPA intervention group (Fig. 7B).

Next, to further study the phylogenetic relationships of species at the genus level, the phylogenetic relationships of the top 100 genera's representative sequences were obtained through multiple sequence alignments (Fig. 7C). Compared with the normal control group, the abundances of *Dubosiella, Staphylococcus* and *Lactobacillus* increased, while *Rikenellaceae_RC9_gut_group, Odoribacter, Alistipes, Prevotella* and *Alloprevotella* decreased in the CCl_4 model group, and IPA intervention alleviated the changes.

Beta diversity showed that the differences in microbial community between the CCl_4 model group and normal control group (0.346 and 0.388, weighted and unweighted respectively) could be reduced (0.198 and 0.292, weighted and unweighted respectively) via intervention with IPA (Supplementary Fig. 1A–C). Furthermore, we used the Rarefaction Curve and Rank Abundance to characterize the diversity of samples. The result showed a massive decrease in the diversity of the microbial community in the feces of the

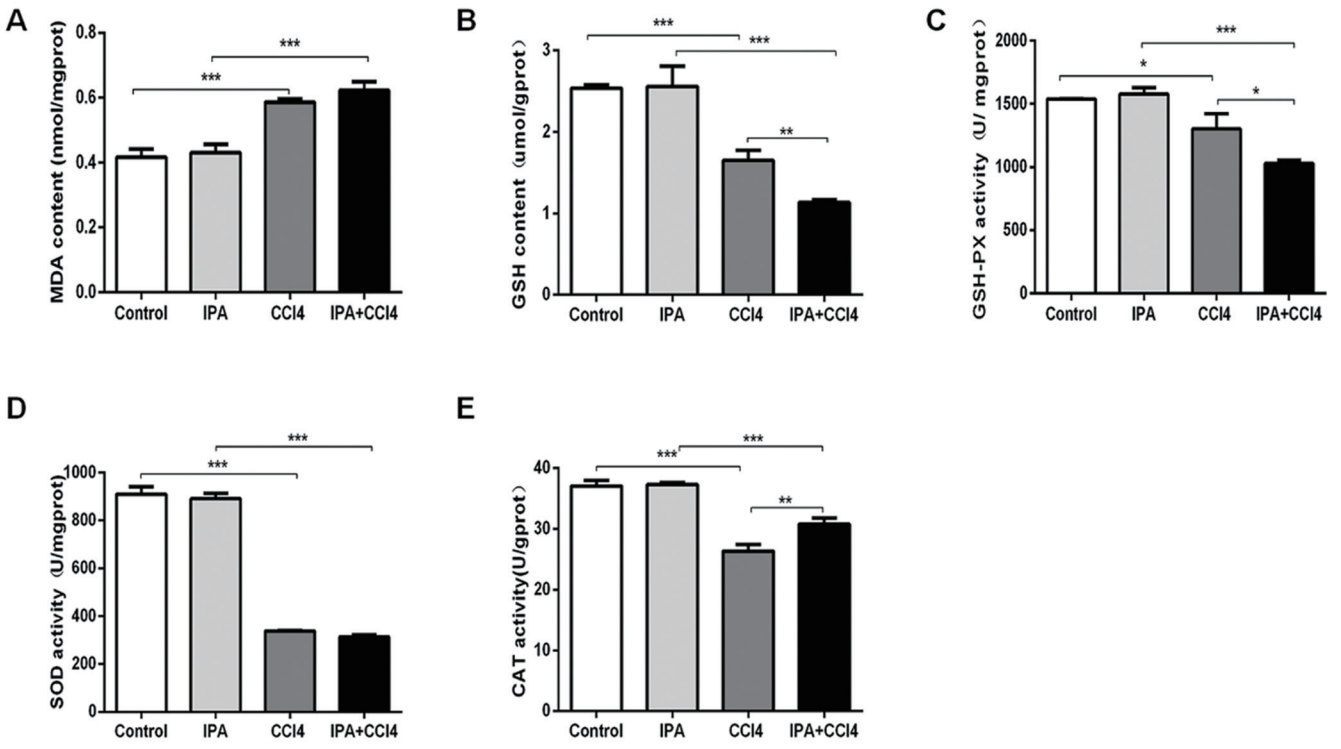

Fig. 3. Effect of IPA intervention on CCl_4-induced hepatic oxidative stress in mice. (A) Content of MDA in the liver. (B) Content of GSH in the liver. (C–E) Activities of GSH-Px, SOD, and CAT in the liver. All values were assessed by two independent experiments; the values represent the mean±SEM. n=3–4. *p<0.05, **p<0.01, ***p<0.001. CAT, catalase; CCl_4, carbon tetrachloride; GSH, glutathione; GSH-PX, glutathione peroxidase; IPA, indole-3-propionate; MDA, malonyldialdehyde; SOD, superoxide dismutase.

mice treated with CCl_4, and oral administration of IPA led to an increase (Fig. 7D–E). Together, these data suggested that repeated intraperitoneal injection of CCl_4 markedly altered the bacterial structure and reduced microbial diversity in the fecal samples, and IPA intervention could alleviate the intestinal flora disorders caused by CCl_4 to a certain extent, but it also significantly altered the composition of gut microbes.

Discussion

Liver fibrosis is a common pathological process of CLD; its pathogenesis involves liver injury, inflammation, oxidative stress, and intestinal dysfunction.[2] IPA is similar in structure to melatonin. More and more studies have confirmed the beneficial effects of IPA on the intestines[30] and liver,[15] which are mainly manifested in stabilizing the intestinal mucosal barrier, regulating the intestinal flora, and interacting with the immune system to change intestinal biology properties, such as anti-inflammatory and anti-oxidant. Although previous research has proposed subtle differences in the chemical structure between melatonin and IPA and speculated the latter substance may have unfavorable effects,[10,17,18] there are no relevant reports so far. In this study, we obtained several unexpected results; specifically, IPA administration seemed to aggravate hepatic injury and liver fibrosis in the CCl_4-induced liver fibrosis model, as evidenced by pathological changes in liver tissue, serum ALT and AST levels, hepatocyte apoptosis rate, and the expression levels of inflammatory cytokines and liver fibrosis-related-genes. Therefore, this research was focused on exploring the reasons and underlying mechanisms of IPA aggravating liver fibrosis (Fig. 8).

There is a broad consensus that the activation of HSCs usually plays a crucial role in the initiation and progression of hepatic fibrosis.[2] In normal liver, HSCs are mainly responsible for storing vitamin A and regulating the blood flow of the liver sinusoids. Once activated, HSCs differentiate into myofibroblasts and express a large amount of α-SMA, collagen I, and TGF-β1, resulting in excessive deposition of ECM,[2] and TGF-β1 can modulate the expression of MMPs and TIMPs.[5,31] Generally, MMPs play an essential role in the degradation of ECM and TIMPs promote ECM synthesis, thereby maintaining the homeostasis of ECM.[32] The dysregulated ECM synthesis and degradation will cause collagen over-deposition and promote liver fibrosis. Consistent with previously reported findings,[33] increased expression of α-SMA, collagen-I, TIMP-1, and MMP-2 occurs in mice treated with IPA plus CCl_4 than CCl_4 alone (Fig. 5), indicating that IPA administration exacerbates CCl_4-induced hepatic fibrosis, possibility through activating the HSCs.

To further investigate the effect of IPA on HSC activation, we detected the critical signaling pathway of TGF-β1/Smads.[7] The results showed that the elevated levels of TGF-β1, Smad3 and p-Smad2/3 in the IPA intervention group were more pronounced than in the CCl_4 model group, while Samd7 was more inhibited (Fig. 6A–C). In the TGF-β/Smads pathway, TGF-β binds with and phosphorylates the TGF-β type II receptor (i.e. TβR II) on the liver cell membrane, then recruits and phosphorylates the TGF-β receptor type I (i.e. TβR I). Finally, the activated TβR I leads to phosphorylation of downstream Smad2 and Smad3, resulting in excessive ECM production.[8] On the other hand, Smad7 can block the over-activation of TGF-β signals by preventing the phosphorylation of R-Smads.[8] Collectively, the above evidence indicates that IPA-promoted ECM formation might

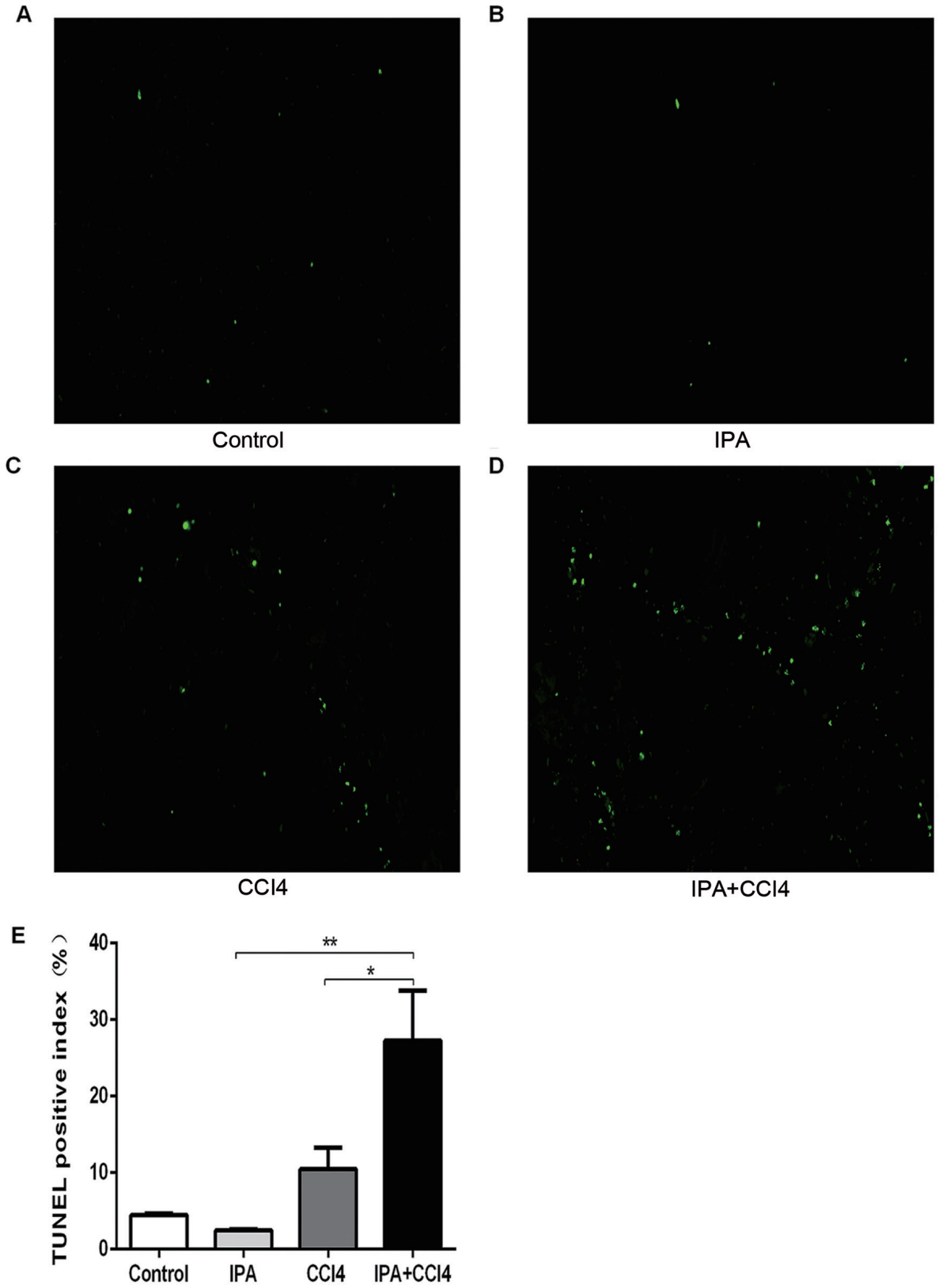

Fig. 4. Effects of IPA on the apoptotic cell. (A–D) TUNEL staining showing apoptotic cells in liver tissue sections (magnification 200×). (E) Quantification of TUNEL staining. n=3-4.*p<0.05, **p<0.01. IPA, indole-3-propionate; TUNEL, terminal deoxynucleotidyl transferase-mediated dUTP nick end labeling.

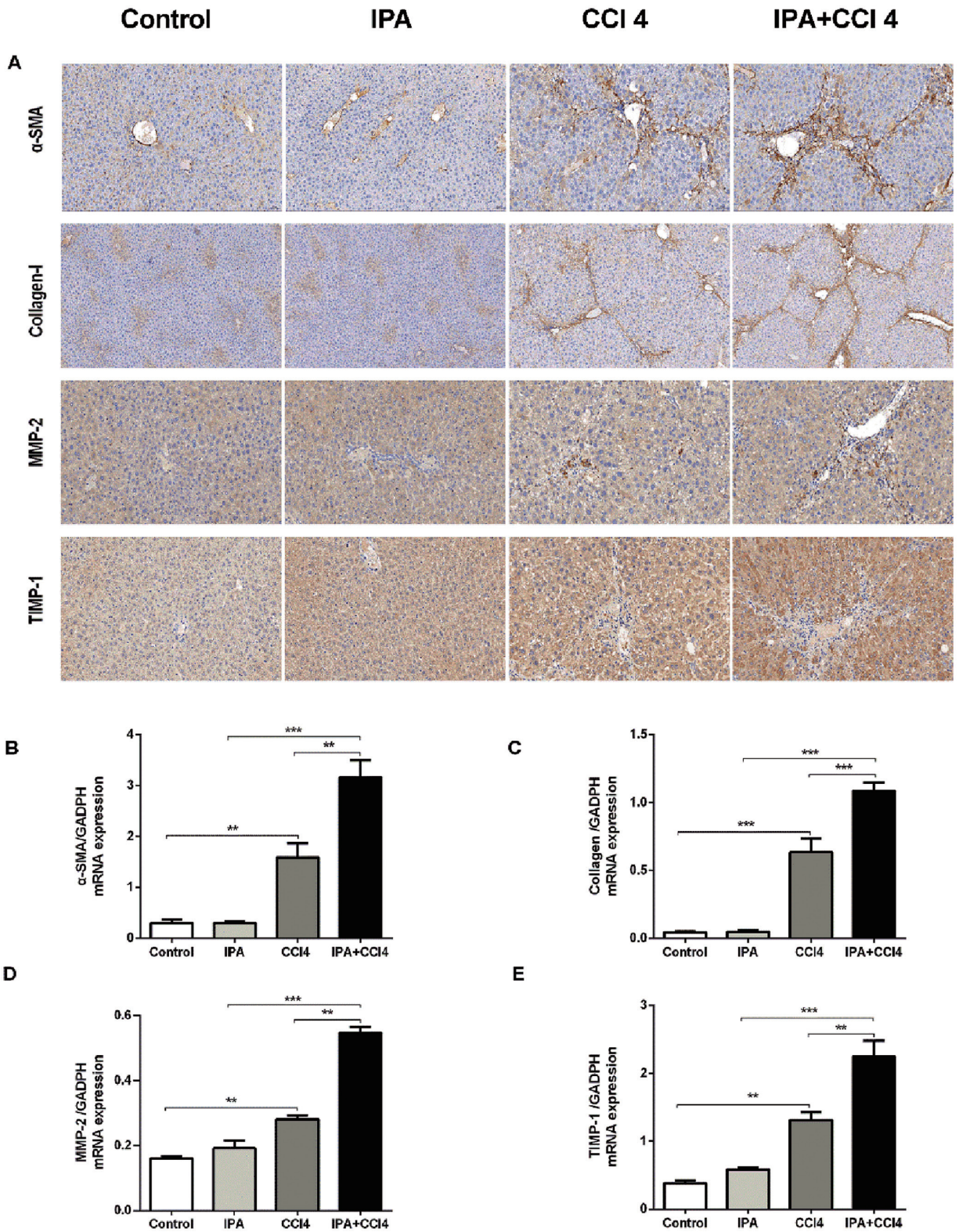

Fig. 5. IPA promoted liver fibrosis by activating the HSCs. (A) IHC staining of α-SMA, collagen-1, MMP-2, and TIMP-1 in the liver tissues (magnification 200×). (B–E) Effects of IPA on the mRNA expression of α-SMA, collagen-1, MMP-2, and TIMP-1 in the liver tissues measured by qPCR. All values were assessed by two independent experiments; the values represent the mean±SEM. n=3-4. *p<0.05, **p<0.01, ***p<0.001. α-SMA, α-smooth muscle actin; HSCs, hepatic stellate cells; IHC, immunohistochemistry; IPA, indole-3-propionate; MMPs, matrix metalloproteinases; qPCR, quantitative real-time polymerase chain reaction; TIMPs, tissue inhibitors of metalloproteinase.

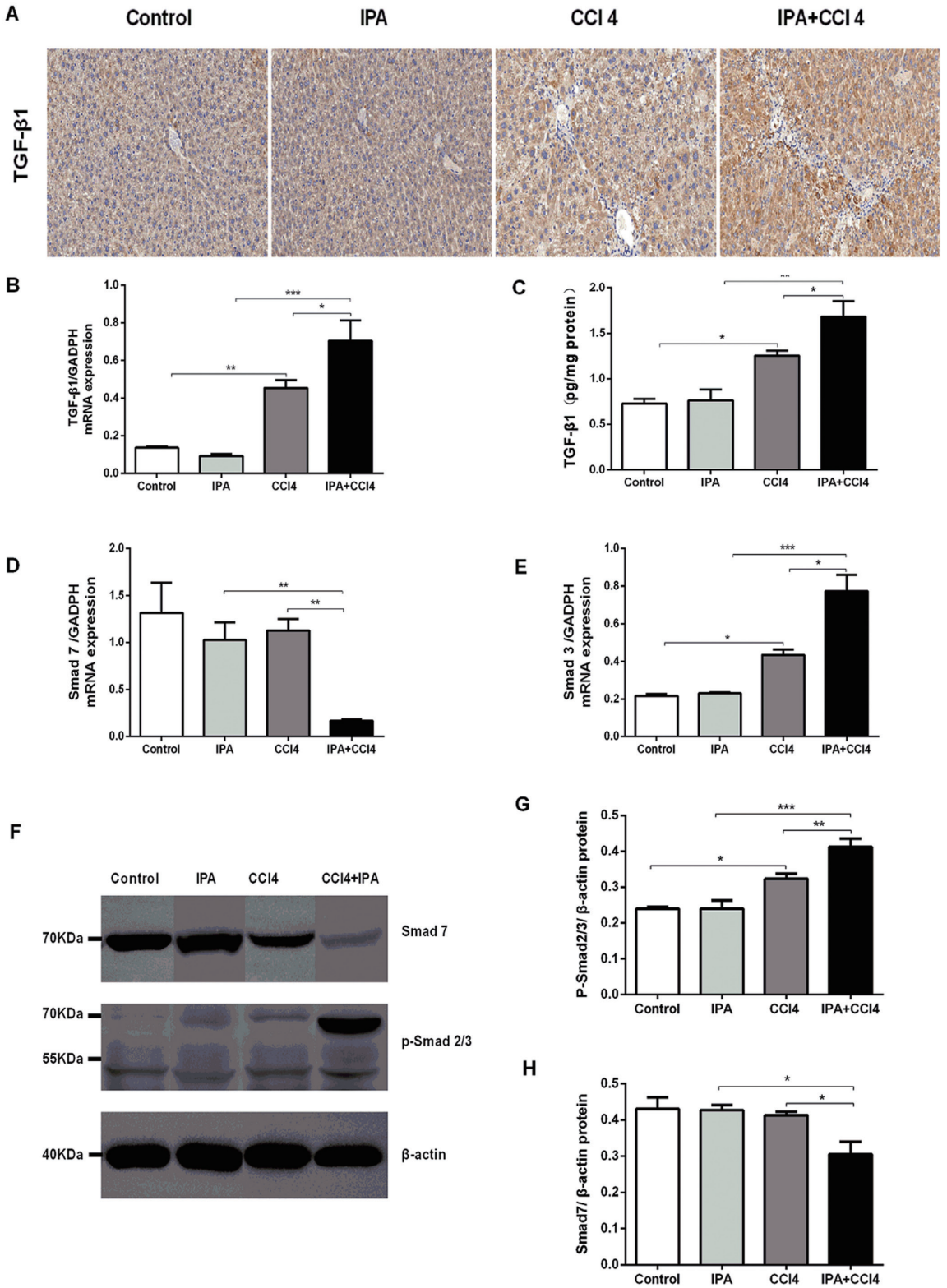

Fig. 6. IPA promotes liver fibrosis via TGF-β1/Smads signaling. (A) IHC staining of TGF-β1 in the liver tissues (magnification 200×). (B) TGF-β1 protein determined by ELISA analysis. (C–E) qPCR-detected TGF-β1, Smad3, and Smad7 mRNA expression. (F) Western blot analysis of p-Smad2/3 and Smad7. (G–H) Protein expression of p-Smad2/3 and Smad7. All values were assessed by two independent experiments; the values represent the mean±SEM. n=3-4. *p<0.05, **p<0.01, ***p<0.001. α-SMA, ELISA, enzyme-linked immunosorbent assay; IHC, immunohistochemistry; IPA, indole-3-propionate; qPCR, quantitative real-time polymerase chain reaction; TGF-β, transforming growth factor-β.

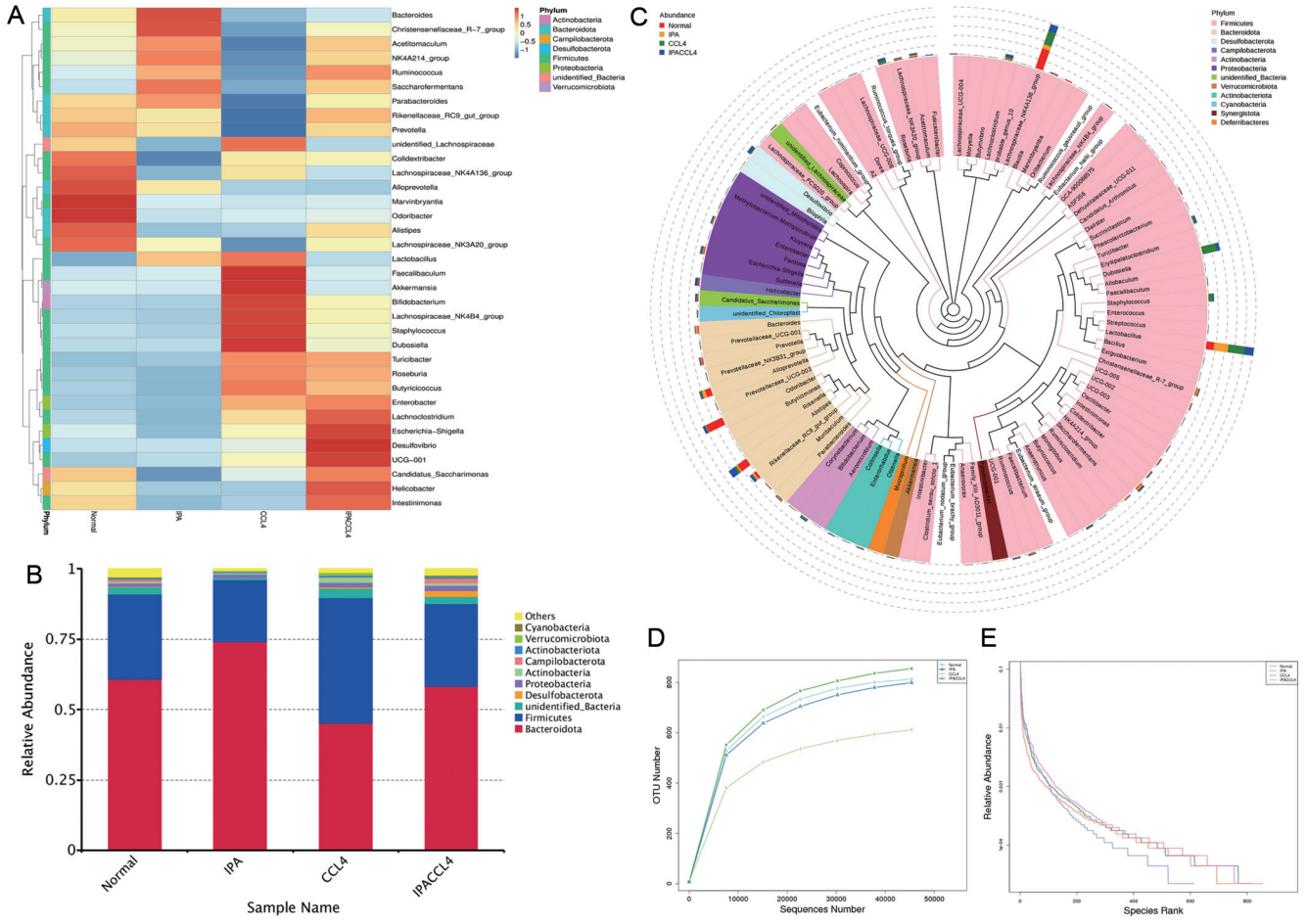

Fig. 7. Effect of oral IPA on gut microbiota in CCl_4-induced liver fibrosis. (A) Species abundance cluster map showing significant changes in expression of relative abundance in genus species level in each group. The vertical direction is the sample information, and the horizontal direction is the species annotation information. The cluster tree on the left of the figure is the species cluster tree; the corresponding value of the heat map is the Z value obtained after the relative abundance of each row of species is standardized. (B) Relative abundance in phylum species level. (C) The phylogenetic relationships of the representative sequences of the top 100 genera were obtained through multiple sequence alignments. The phylogenetic tree is constructed by the representative sequence of the species at the genus level, the color of the branch indicates its corresponding phylum, and each color represents a phylum. (D) Rarefaction Curve: the abscissa is the number of sequenced samples randomly selected from a sample, and the ordinate is the number of OTUs that can be constructed based on the number of sequenced samples, which is used to reflect the depth of sequencing. Curves with different colors represent different samples. (E) Rank Abundance: The abscissa is the serial number sorted by the abundance of OTUs, and the ordinate is the relative abundance of the corresponding OTUs. Broken lines with different colors represent different samples. CCl_4, carbon tetrachloride; ELISA, enzyme-linked immunosorbent assay; IL, interleukin; IPA, indole-3-propionate; OTUs, Operational Taxonomic Units.

occur by activating HSCs via the TGF-β1/Smads signaling pathway. Additionally, TGF-β can induce hepatocyte apoptosis;[34] thus, the increased hepatocyte apoptosis in the IPA intervention group verified the above conclusion again.

Oxidative stress and inflammation have been considered the major causative factor of liver damage.[4] With sustained exposure to CCl_4, ROS accumulates in the liver and the activity of antioxidant enzymatic (SOD, CAT, and GSH-Px) decreases, thus leading to hepatocyte necrosis and apoptosis.[35] Besides, ROS can activate HSCs and act as both inducer and effector of the TGF-β signaling pathway.[36] According to reports, IPA can scavenge free radicals and protect the liver from oxidative damage.[18] However, the results of this study found that IPA administration decreased the levels of GSH and GSH-Px in liver tissue, besides increasing the activity of CAT to a certain extent. The level of MDA content showed no significant difference between the CCl_4 model and the IPA intervention groups; although, another study found that IPA was relatively potent in preventing hydrogen peroxide-induced, hydroxyl radical-mediated formation of MDA.[17] In summary, we have not found evidence that IPA can protect against oxidative stress-induced by CCl_4. After all, IPA is a poor chain-breaking antioxidant and would reduce lipid peroxidation effectively only when used at a high pharmacological concentration.[17,18] One possible reason for this may be that the concentration of IPA in this experiment did not reach the minimum concentration required to eliminate the oxidative stress induced by CCl_4. Another possible reason may be related to IPA's direct pro-oxidative effect on membrane fluidity via influencing the composition of the membranes.[18] The underlying mechanisms still needs further elucidation.

It has been shown that intraperitoneal injection of CCl_4 can induce hepatocyte inflammatory response, which is manifested by increased TNF-α, IL-6, IL-8, IL-1β, and IL-10.[37] Moreover, IL-6, IL-8, and IL-1β are increased following CCl_4-induced TNF-α release.[37,38] Among these inflammatory mediators, pro-inflammatory cytokines including TNF-α, IL-8, IL-1β, and IL-6 play an important role in the activation of HSCs and synthesis of ECM.[37,39] IL-10 acts as an anti-

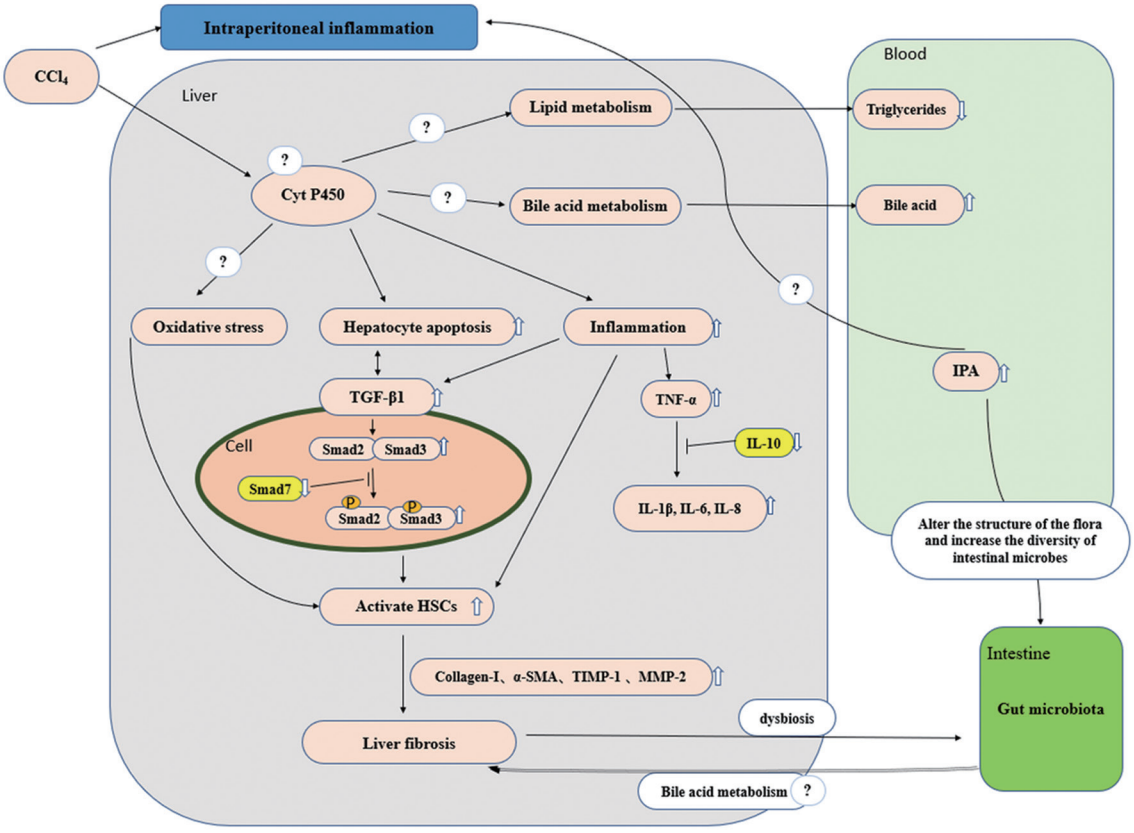

Fig. 8. Mechanism of IPA on CCl_4-induced liver fibrosis. Administration of IPA enhanced CCl_4-induced liver fibrosis via activating HSCs and the TGF-β1/Smads signaling pathway. Moreover, IPA aggravated liver inflammation and increased hepatocytes apoptosis. Furthermore, IPA altered the structure of the flora and increased the diversity of intestinal microbes. There are issues not yet clear and need to be studied further: 1) Whether IPA affects the activity of cytochrome P450? 2) Whether the intra-abdominal inflammatory reaction induced by intraperitoneal CCl_4 administration interacts with IPA administration? 3) Whether the result of enhanced liver fibrosis is related to the impact of IPA on intestinal flora? 4) How IPA acts on oxidative stress induced by CCl_4? 5) How IPA affects bile acid metabolism? 6) How IPA affects lipid metabolism? CCl_4, carbon tetrachloride; IPA, indole-3-propionate; HSCs, hepatic stellate cells; TGF-β, transforming growth factor-β.

inflammatory and antifibrotic mediator.[40] Higher levels of proinflammatory cytokines and lower levels of anti-inflammatory cytokines seem to partly explain the phenomenon that IPA-aggravated liver fibrosis in this investigation. It has been confirmed that IPA can attenuate hepatic inflammation and liver injury of NAFLD by inhibiting LPS-mediated toll-like receptor 4/NF-κB signaling.[15] It is still unclear why IPA exacerbated the inflammation response in mice treated with CCl_4.

Gut bacterial dysbiosis is also associated with worsening of the liver disease.[41] Liver fibrosis is often accompanied by dysbacteriosis and bacterial translocation,[42] As previously described,[15] our study also showed that IPA intervention can increase the diversity of intestinal microbes and reduce the *Firmicutes* to *Bacteroidetes* ratio. However, it increased the abundance of *Desulfobacteraceae*, *Campilobacteriacea*, *Odoribacter, Helicobacter* and *Alistipes*, as well as decreased the abundance of *Lactobacillus* (Fig. 7B–C). Among these genera, *Odoribacter* is implied to be important for intestinal homeostasis[15] and *Alistipes* shows a decrease in the process of liver fibrosis.[43] This indicated that IPA intervention could alleviate the gut microbiota dysbiosis induced by CCl_4 to a certain extent. However, *Desulfobacteraceae* is a pro-inflammatory bacteria that can cause more inflammatory cytokine responses[28] and has been reported to be associated with inflammatory bowel disease.[44] Additionally, *Campylobacteraceae* is a leading cause of bacterial enteritis, stimulating the pro-inflammatory pathway and the production of a large repertoire of cytokines, chemokines, and innate effector molecules.[29] Moreover, *Helicobacter* has been reported as having a positive association with HCC.[45] Recent studies have found that intestinal diseases can aggravate liver fibrosis through the "gut-liver axis".[46] The "gut-liver axis" theory suggests that there is an interaction between the gut and its microbiota and the liver.[9] The liver participates in the composition and metabolism of intestinal microbes through enterohepatic circulation (referred to as EHC), thereby affecting intestinal health. At the same time, changes in intestinal factors and microbiota exposed to the liver also affect liver inflammation and damage during CLD. Whether the increased abundance of pathogenic bacteria is the cause of IPA-exacerbated CCl_4-induced liver fibrosis remains to be further studied.

Furthermore, the gut microbiota can modulate bile acid metabolism,[47] and *Lactobacillus* has been proven to regulate the expression of hepatic genes involved in bile acid homeostasis and promote fecal excretion of intestinal bile acids.[44] Attractively, the total serum bile acid level, the primary endogenous substance of EHC, in the IPA intervention group was significantly higher than that in the CCl_4 model group in this study (Fig. 1L). Metabolomics studies have found that bile acids can regulate the relationship between the intestinal flora and the liver, and affect the progress of CLD.[48] Moreover, excessive accumulation of bile acids in the liver can lead to liver injuries by triggering inflammatory responses.[47,49] Thus, the possible mechanism by which IPA

intervention can enhance inflammation might be related to changes in bile acid metabolism. Specifically, in the condition of gut microbiota dysbiosis in mice with CCl_4-induced fibrosis, oral IPA might increase reabsorption of bile acids via altering intestinal flora structure, thereby strengthening liver inflammation and promoting liver fibrosis. However, this assumption still needs more in-depth research.

Overall, in contrast with previous research,[15,50] our study showed that IPA might, via activating HSCs and the TGF-β1/Smads signaling pathway, aggravate liver inflammation and increase hepatocyte apoptosis to significantly enhanced CCl_4-induced liver injury and fibrosis. However, there remain several problems that need to be solved in further research. Firstly, IPA alone does not stimulate hepatotoxic effects and even has been recognized as a beneficial compound in other animal models; thus, it would be helpful to understand how IPA aggravates liver fibrosis if it were commenced later during CCl_4 exposure, i.e. in animals with well-established fibrosis. Second, how IPA increases the toxicity of CCl_4 remains unclear; potential impact mechanisms include (but are not limited to): 1) Whether IPA increases the acute toxicity of CCl_4? 2) Whether IPA affects the activity of cytochrome P450, the main metabolic enzyme of CCl_4? 3) Whether the intra-abdominal inflammatory reaction induced by intraperitoneal CCl_4 administration interacts with IPA administration? 4) Whether the species and strains of experimental animals affect the research results? Besides, the power of the study was reduced by the relatively small number of mice used, but the difference between the experimental group and the control group is very significant, especially in the performance of histopathology, and we obtained the same results in two independently repeated experiments; thus, the conclusion of this study is credible to a certain extent.

Funding

This work received financial support from the Scientific Research Project of Sichuan Provincial Health and Family Planning Commission (No. 18PJ340), Luzhou Municipal People's Government-Southwest Medical University Science and Technology Strategic Cooperation Applied Basic Research Project (No. 2018LZXNYD-ZK29), Scientific Research Project for Young Researchers of Southwest Medical University (No. 2017-ZRQN-103), Affiliated Hospital of Southwest Medical University Research Grant (No. 16237), and Sichuan Provincial Department of Health (No. 12094).

Conflict of interest

The authors have no conflict of interests related to this publication.

Author contributions

Conception of the study (GW, CS), experimental design (CS, FL), data curation (FL, YC), data collection (FL, YY, FD), reference collection and writing-original draft (FL), manuscript modification (GW, CS), and funding acquisition (GW, CS). All authors contributed to and approved the final manuscript.

Data sharing statement

The data used to support the findings of this study are available from the corresponding author upon request. The readers can contact Professor Wu via email (email address: wugang2020@swmu.edu.cn) to obtain data.

References

[1] Shan L, Liu Z, Ci L, Shuai C, Lv X, Li J. Research progress on the anti-hepatic fibrosis action and mechanism of natural products. Int Immunopharmacol 2019;75:105765. doi:10.1016/j.intimp.2019.105765.
[2] Higashi T, Friedman SL, Hoshida Y. Hepatic stellate cells as key target in liver fibrosis. Adv Drug Deliv Rev 2017;121:27–42. doi:10.1016/j.addr.2017.05.007.
[3] Roeb E. Matrix metalloproteinases and liver fibrosis (translational aspects). Matrix Biol 2018;68-69:463–473. doi:10.1016/j.matbio.2017.12.012.
[4] Li S, Hong M, Tan HY, Wang N, Feng Y. Insights into the role and interdependence of oxidative stress and inflammation in liver diseases. Oxid Med Cell Longev 2016;2016:4234061. doi:10.1155/2016/4234061.
[5] Fabregat I, Caballero-Diaz D. Transforming growth factor-beta-induced cell plasticity in liver fibrosis and hepatocarcinogenesis. Front Oncol 2018;8:357. doi:10.3389/fonc.2018.00357.
[6] Parola M, Pinzani M. Liver fibrosis: pathophysiology, pathogenetic targets and clinical issues. Mol Aspects Med 2019;65:37–55. doi:10.1016/j.mam.2018.09.002.
[7] Dewidar B, Meyer C, Dooley S, Meindl-Beinker AN. TGF-beta in hepatic stellate cell activation and liver fibrogenesis-updated 2019. Cells 2019;8(11):1419. doi:10.3390/cells8111419.
[8] Xu F, Liu C, Zhou D, Zhang L. TGF-beta/SMAD pathway and its regulation in hepatic fibrosis. J Histochem Cytochem 2016;64(3):157–167. doi:10.1369/0022155415627681.
[9] Yu LX, Schwabe RF. The gut microbiome and liver cancer: mechanisms and clinical translation. Nat Rev Gastroenterol Hepatol 2017;14(9):527–539. doi:10.1038/nrgastro.2017.72.
[10] Karbownik M, Stasiak M, Zygmunt A, Zasada K, Lewiński A. Protective effects of melatonin and indole-3-propionic acid against lipid peroxidation, caused by potassium bromate in the rat kidney. Cell Biochem Funct 2006;24(6):483–489. doi:10.1002/cbf.1321.
[11] Chyan YJ, Poeggeler B, Omar RA, Chain DG, Frangione B, Ghiso J, *et al*. Potent neuroprotective properties against the Alzheimer beta-amyloid by an endogenous melatonin-related indole structure, indole-3-propionic acid. J Biol Chem 1999;274(31):21937–21942. doi:10.1074/jbc.274.31.21937.
[12] Sári Z, Mikó E, Kovács T, Jankó L, Csonka T, Lente G, *et al*. Indolepropionic acid, a metabolite of the microbiome, has cytostatic properties in breast cancer by activating AHR and PXR receptors and inducing oxidative stress. Cancers (Basel) 2020;12(9):2411. doi:10.3390/cancers12092411.
[13] Dodd D, Spitzer MH, Van Treuren W, Merrill BD, Hryckowian AJ, Higginbottom SK, *et al*. A gut bacterial pathway metabolizes aromatic amino acids into nine circulating metabolites. Nature 2017;551(7682):648–652. doi:10.1038/nature24661.
[14] Venkatesh M, Mukherjee S, Wang H, Li H, Sun K, Benechet AP, *et al*. Symbiotic bacterial metabolites regulate gastrointestinal barrier function via the xenobiotic sensor PXR and Toll-like receptor 4. Immunity 2014;41(2):296–310. doi:10.1016/j.immuni.2014.06.014.
[15] Zhao ZH, Xin FZ, Xue Y, Hu Z, Han Y, Ma F, *et al*. Indole-3-propionic acid inhibits gut dysbiosis and endotoxin leakage to attenuate steatohepatitis in rats. Exp Mol Med 2019;51(9):103. doi:10.1038/s12276-019-0304-5.
[16] Roager HM, Licht TR. Microbial tryptophan catabolites in health and disease. Nat Commun 2018;9(1):3294. doi:10.1038/s41467-018-05470-4.
[17] Poeggeler B, Pappolla MA, Hardeland R, Rassoulpour A, Hodgkins PS, Guidetti P, *et al*. Indole-3-propionate: a potent hydroxyl radical scavenger in rat brain. Brain Res 1999;815(2):382–388. doi:10.1016/s0006-8993(98)01027-0.
[18] Karbownik M, Reiter RJ, Garcia JJ, Cabrera J, Burkhardt S, Osuna C, *et al*. Indole-3-propionic acid, a melatonin-related molecule, protects hepatic microsomal membranes from iron-induced oxidative damage: relevance to cancer reduction. J Cell Biochem 2001;81(3):507–513.
[19] Scholten D, Trebicka J, Liedtke C, Weiskirchen R. The carbon tetrachloride model in mice. Lab Anim 2015;49(1 Suppl):4–11. doi:10.1177/0023677215571192.
[20] He W, Zhuang Y, Wang L, Qi L, Chen B, Wang M, *et al*. Geranylgeranylacetone attenuates hepatic fibrosis by increasing the expression of heat shock protein 70. Mol Med Rep 2015;12(4):4895–4900. doi:10.3892/mmr.2015.4069.
[21] Ishak K, Baptista A, Bianchi L, Callea F, De Groote J, Gudat F, *et al*. Histological grading and staging of chronic hepatitis. J Hepatol 1995;22(6):696–699. doi:10.1016/0168-8278(95)80226-6.
[22] Kyrylkova K, Kyryachenko S, Leid M, Kioussi C. Detection of apoptosis by TUNEL assay. Methods Mol Biol 2012;887:41–47. doi:10.1007/978-1-61779-860-3_5.
[23] Cito G, Coccia ME, Salvianti F, Fucci R, Picone R, Giachini C, *et al*. Blood plasma miR-20a-5p expression as a potential non-invasive diagnostic biomarker of male infertility: a pilot study. Andrology 2020;8(5):1256–1264. doi:10.1111/andr.12816.
[24] Kang Z, Lu M, Jiang M, Zhou D, Huang H. Proteobacteria acts as a pathogenic risk-factor for chronic abdominal pain and diarrhea in post-cholecystectomy syndrome patients: a gut microbiome metabolomics study. Med Sci Monit 2019;25:7312–7320. doi:10.12659/MSM.915984.
[25] Wang Q, Garrity GM, Tiedje JM, Cole JR. Naive Bayesian classifier for rapid assignment of rRNA sequences into the new bacterial taxonomy. Appl Environ Microbiol 2007;73(16):5261–5267. doi:10.1128/AEM.00062-07.

[26] Edgar RC. UPARSE: highly accurate OTU sequences from microbial amplicon reads. Nat Methods 2013;10(10):996–998. doi:10.1038/nmeth.2604.
[27] Kumar S, Wang J, Shanmukhappa SK, Gandhi CR. Toll-like receptor 4-independent carbon tetrachloride-induced fibrosis and lipopolysaccharide-induced acute liver injury in mice: role of hepatic stellate cells. Am J Pathol 2017;187(6):1356–1367. doi:10.1016/j.ajpath.2017.01.021.
[28] Bromberg JS, Hittle L, Xiong Y, Saxena V, Smyth EM, Li L, *et al*. Gut microbiota-dependent modulation of innate immunity and lymph node remodeling affects cardiac allograft outcomes. JCI Insight 2018;3(19):e121045. doi:10.1172/jci.insight.121045.
[29] van Putten JP, van Alphen LB, Wösten MM, de Zoete MR. Molecular mechanisms of campylobacter infection. Curr Top Microbiol Immunol 2009;337:197–229. doi:10.1007/978-3-642-01846-6_7.
[30] Li J, Zhang L, Wu T, Li Y, Zhou X, Ruan Z. Indole-3-propionic acid improved the iIntestinal barrier by enhancing epithelial barrier and mucus barrier. J Agric Food Chem 2021;69(5):1487–1495. doi:10.1021/acs.jafc.0c05205.
[31] Sentíes-Gómez MD, Gálvez-Gastélum FJ, Meza-García E, Armendáriz-Borunda J. Fibrosis hepática. El papel de las metaloproteinasas y de TGF-beta [Hepatic fibrosis: role of matrix metalloproteases and TGFbeta]. Gac Med Mex 2005;141(4):315–322.
[32] Elpek GÖ. Cellular and molecular mechanisms in the pathogenesis of liver fibrosis: an update. World J Gastroenterol 2014;20(23):7260–7276. doi:10.3748/wjg.v20.i23.7260.
[33] Turkseven S, Bolognesi M, Brocca A, Pesce P, Angeli P, Di Pascoli M. Mitochondria-targeted antioxidant mitoquinone attenuates liver inflammation and fibrosis in cirrhotic rats. Am J Physiol Gastrointest Liver Physiol 2020;318(2):G298–G304. doi:10.1152/ajpgi.00135.2019.
[34] Shrestha N, Chand L, Han MK, Lee SO, Kim CY, Jeong YJ. Glutamine inhibits CCl4 induced liver fibrosis in mice and TGF-beta1 mediated epithelial-mesenchymal transition in mouse hepatocytes. Food Chem Toxicol 2016;93:129–137. doi:10.1016/j.fct.2016.04.024.
[35] Lahera V, Goicoechea M, de Vinuesa SG, Oubina P, Cachofeiro V, Gomez-Campdera F, *et al*. Oxidative stress in uremia: the role of anemia correction. J Am Soc Nephrol 2006;17(12 Suppl 3):S174–177. doi:10.1681/ASN.2006080911.
[36] Lin W, Tsai WL, Shao RX, Wu G, Peng LF, Barlow LL, *et al*. Hepatitis C virus regulates transforming growth factor beta1 production through the generation of reactive oxygen species in a nuclear factor kappaB-dependent manner. Gastroenterology 2010;138(7):2509–2518, 2518.e1doi:10.1053/j.gastro.2010.03.008.
[37] Weber LW, Boll M, Stampfl A. Hepatotoxicity and mechanism of action of haloalkanes: carbon tetrachloride as a toxicological model. Crit Rev Toxicol 2003;33(2):105–136. doi:10.1080/713611034.
[38] Beringer A, Miossec P. IL-17 and TNF-α co-operation contributes to the pro-inflammatory response of hepatic stellate cells. Clin Exp Immunol 2019;198(1):111–120. doi:10.1111/cei.13316.
[39] Gomez-Hurtado I, Santacruz A, Peiro G, Zapater P, Gutierrez A, Perez-Mateo M, *et al*. Gut microbiota dysbiosis is associated with inflammation and bacterial translocation in mice with CCl4-induced fibrosis. PLoS One 2011;6(7):e23037. doi:10.1371/journal.pone.0023037.
[40] Xu Y, Tang X, Yang M, Zhang S, Li S, Chen Y, *et al*. Interleukin 10 gene-modified bone marrow-derived dendritic cells attenuate liver fibrosis in mice by inducing regulatory T cells and inhibiting the TGF-*β*/Smad signaling pathway. Mediators Inflamm 2019;2019:4652596. doi:10.1155/2019/4652596.
[41] Albhaisi SAM, Bajaj JS, Sanyal AJ. Role of gut microbiota in liver disease. Am J Physiol Gastrointest Liver Physiol 2020;318(1):G84–G98. doi:10.1152/ajpgi.00118.2019.
[42] Mazagova M, Wang L, Anfora AT, Wissmueller M, Lesley SA, Miyamoto Y, *et al*. Commensal microbiota is hepatoprotective and prevents liver fibrosis in mice. FASEB J 2015;29(3):1043–1055. doi:10.1096/fj.14-259515.
[43] Parker BJ, Wearsch PA, Veloo ACM, Rodriguez-Palacios A. The genus alistipes: gut bacteria with emerging implications to inflammation, cancer, and mental health. Front Immunol 2020;11:906. doi:10.3389/fimmu.2020.00906.
[44] Lv XC, Chen M, Huang ZR, Guo WL, Ai LZ, Bai WD, *et al*. Potential mechanisms underlying the ameliorative effect of Lactobacillus paracasei FZU103 on the lipid metabolism in hyperlipidemic mice fed a high-fat diet. Food Res Int 2021;139:109956. doi:10.1016/j.foodres.2020.109956.
[45] Okushin K, Tsutsumi T, Ikeuchi K, Kado A, Enooku K, Fujinaga H, *et al*. *Helicobacter pylori* infection and liver diseases: epidemiology and insights into pathogenesis. World J Gastroenterol 2018;24(32):3617–3625. doi:10.3748/wjg.v24.i32.3617.
[46] Tian Y, Li Y, Wang WX, Jiang WL, Fei J, Li CY. Novel strategy for validating the existence and mechanism of the "gut-liver axis" in vivo by a hypoxia-sensitive NIR fluorescent probe. Anal Chem 2020;92(6):4244–4250. doi:10.1021/acs.analchem.9b04578.
[47] Chiang JYL, Ferrell JM. Bile acid metabolism in liver pathobiology. Gene Expr 2018;18(2):71–87. doi:10.3727/105221618X15156018385515.
[48] Chopyk DM, Grakoui A. Contribution of the intestinal microbiome and gut barrier to hepatic disorders. Gastroenterology 2020;159(3):849–863. doi:10.1053/j.gastro.2020.04.077.
[49] Chen ML, Takeda K, Sundrud MS. Emerging roles of bile acids in mucosal immunity and inflammation. Mucosal Immunol 2019;12(4):851–861. doi:10.1038/s41385-019-0162-4.
[50] Hendrikx T, Schnabl B. Indoles: metabolites produced by intestinal bacteria capable of controlling liver disease manifestation. J Intern Med 2019;286(1):32–40. doi:10.1111/joim.12892.